Journal of Hydrology 661 (2025) 133607

Contents lists available at ScienceDirect

Journal of Hydrology

journal homepage: www.elsevier.com/locate/jhydrol

Future precipitation extremes and urban flood risk assessment using a non-stationary and convection-permitting climate-hydrodynamic modeling framework

Patrick Laux [a,b,*], David Feldmann [a,c], Francesco Marra [d], Hendrik Feldmann [e], Harald Kunstmann [a,b], Katja Trachte [f], Nadav Peleg [g,h]

[a] Campus Alpin, Karlsruhe Institute of Technology (KIT), Kreuzeckbahnstraße 19, Garmisch-Partenkirchen, 82467, Germany
[b] Institute of Geography, University of Augsburg, Alter Postweg 118, Augsburg, 86159, Germany
[c] Dr. Blasy - Dr. Øverland Ingenieure GmbH, Billerberg 10, Inning am Ammersee, 82266, Germany
[d] Department of Geosciences, University of Padova, Via Gradenigo 6, Padova, 35131, Italy
[e] Institute of Meteorology and Climate Research Troposphere Research (IMKTRO), Karlsruhe Institute of Technology (KIT), POB 3640, Karlsruhe, 76021, Germany
[f] Department of Atmospheric Processes, Brandenburg University of Technology Cottbus-Senftenberg, Burger Chaussee 2, Cottbus, 03044, Germany
[g] Institute of Earth Surface Dynamics, University of Lausanne, UNIL-Mouline, Lausanne, 1015, Switzerland
[h] Expertise Center for Climate Extremes, University of Lausanne, UNIL-Mouline, Lausanne, 1015, Switzerland

ARTICLE INFO

This manuscript was handled by Yuefei Huang, Editor-in-Chief, with the assistance of Mingfu Guan, Associate Editor.

Dataset link: https://www-regiklim.dkrz.de/?login_required=1&next=/solr/data-browser/%3Fproduct%3Dceu-3%26project%3Dnukleus, https://opendata.dwd.de/climate_environment/CDC/, https://www.wdc-climate.de/ui/entry?acronym=PrecExtr100yr, https://doi.org/10.5281/zenodo.8332232, https://doi.org/10.5281/zenodo.3971557

Keywords:
Urban pluvial flooding
Non-stationary precipitation extremes
Clausius-Clapeyron
TENAX
Convection-permitting models
Hydrodynamic modeling
Flood hazard

ABSTRACT

Urban planners and engineers rely on historical climate data to plan and design flood protection infrastructure that should withstand extreme flooding events with 1% annual exceedance probability (the 100-year flood). Here, we examine how hourly precipitation extremes are expected to change as temperatures rise and how this will affect urban flooding. The changes to short-duration rainfall extremes, often insufficiently considered in practice, are addressed utilizing a new temperature conditional extreme precipitation scaling approach and a novel regional climate convection-permitting model ensemble for +2 °C and +3 °C global warming scenarios. Based on hydrodynamic modeling, we estimate how future precipitation extremes translate into flood risks in two pre-alpine communes in Germany. Ignoring the impacts of climate change may lead to severe underestimations of flood risks. The +3 °C global warming scenario translates into an increase of 60% of affected buildings by the highest flood risk category (water level of 1 m and above). The increase in flow intensities will be greater in the commune characterized by steeper terrain. The results suggest that recently planned or implemented infrastructure projects may not be adequately equipped to cope with the anticipated effects of climate change in the coming decades.

1. Introduction

Recently, Europe experienced several natural disasters that dramatically damaged national economies and insurance companies (Kron et al., 2019). Amongst others, severe convective thunderstorms, which typically occur during the summer and autumn seasons on local spatial scales, associated with strong winds, hail, lightning, and high-intensity precipitation, trigger many pluvial (flash) floods, which are particularly hazardous in inhabited (urban) areas since they generate high runoff volumes that exceed the capacity of drainage systems (Samela et al., 2020). For example, in May and June 2016, Baden-Wuerttemberg and Bavaria, in southern Germany, witnessed severe flooding due to numerous heavy convective storms, with precipitation intensities that exceeded 100 mm within a few hours; e.g., the Braunsbach flood event (Baden-Wuerttemberg) was initiated by approximately 130 mm that fell within 2 h (Bronstert et al., 2018). These events added to damages of 2.2 billion US$ (Kron et al., 2019; Piper et al., 2016).

* Corresponding author at: Campus Alpin, Karlsruhe Institute of Technology (KIT), Kreuzeckbahnstraße 19, Garmisch-Partenkirchen, 82467, Germany.
E-mail address: patrick.laux@kit.edu (P. Laux).

https://doi.org/10.1016/j.jhydrol.2025.133607
Received 18 December 2024; Received in revised form 15 April 2025; Accepted 25 May 2025
Available online 16 June 2025

Another extreme short-term convective precipitation event occurred on the evening of July 24–25th, 2020, in Zagreb, Croatia. A severe thunderstorm resulted in one of the most significant flash floods in Croatia's recorded history. During this event, an episode of intense rainfall delivered locally over 70 mm of precipitation within two hours, corresponding to a return period higher than 100 years. The excessive runoff from the surrounding mountain terrain overwhelmed Zagreb's sewer system, leading to severe urban flooding (Nimac et al., 2022). Similarly, on August 2nd, 2014, a severe thunderstorm hit a summer festival in the Italian Prealps. Over 200 mm of rainfall fell in about two hours, leading to a flash flood that killed four people and injured many more (Borga et al., 2019).

Such convective extreme precipitation events are expected to become more intense with continued global warming due to the increase in the atmospheric water vapor holding capacity described by the Clausius-Clapeyron (C–C) equation, which states that the atmospheric saturation vapor pressure, which quantifies the capacity of the atmosphere to hold moisture before saturation, increases by approximately 7% $°C^{-1}$ (Trenberth et al., 2003; Ludwig et al., 2023). At the sub-daily scale, precipitation maxima may even increase at rates higher than C–C due to temperature-induced changes in local dynamics, referred to as Super C–C scaling (Guerreiro et al., 2018; Fowler et al., 2021a; Da Silva and Haerter, 2023).

Several studies have confirmed trends of extreme precipitation events over short durations (minute to hourly scales) based on observations, some of them approximately following C–C scaling rates across various regions in Europe (Bürger and Bronstert, 2014; Dallan et al., 2022; Persiano et al., 2020). Since urban catchment flooding is primarily driven by precipitation, it is anticipated to worsen with rising temperatures (Sharma et al., 2018; Peleg et al., 2022). This trend highlights the growing climate non-stationarity, emphasizing the urgent need to update the design parameters for precipitation extremes (design storms) – particularly Intensity-Duration-Frequency (IDF) curves (Hosseinzadehtalaei et al., 2020). Such updates are essential to enhance urban infrastructure resilience and improve the accuracy of flood risk assessments (Masson-Delmotte et al., 2021). For example, in the city of Zurich (Switzerland), Peleg et al. (2024) recently derived inundation maps based on future design storms using the Temperature-dependent Non-Asymptotic statistical model for eXtreme return levels (TENAX) model (Marra et al., 2024), statistics from the Euro-CORDEX multi-model ensemble, and the CAFlood hydrodynamic model.

On regional scales (e.g., Europe), systematic design storm updates are very difficult to achieve due to restrictions in the availability of precipitation data. Long-term observation networks on sub-daily scales are usually too sparsely distributed to "observe" small spatial and temporal scales of flash floods (Amponsah et al., 2018; Lengfeld et al., 2020). Radar-based precipitation estimates and observations alone, however, might be inadequate to reflect potentially evolving dynamics and increasing variability in extreme weather patterns in the future climate (Milly et al., 2008). Regional Climate Model (RCM) simulations, and, in particular, very high-resolution (i.e., at kilometer- and sub-hourly spatiotemporal scales) climate simulations using convection-permitting models (CPMs), may provide a suitable alternative to simulate changing extreme weather patterns in the future (Prein et al., 2017). Compared to using RCM output from the EURO-CORDEX project (Hosseinzadehtalaei et al., 2018), CPMs allow us to explicitly resolve the deep convection processes, represent local storm dynamics more realistically, and are thus expected to represent the magnitude of short duration (sub-daily) precipitation extremes more skillfully than non-CPM simulations (Berthou et al., 2020; Fosser et al., 2024). Due to their very high computational demands, CPMs are currently restricted to both shorter simulation periods and relatively small domains (Clark et al., 2016), and if their output is applied to derive IDF values based on classical extreme value theory, large uncertainties can arise (Poschlod, 2021; Dallan et al., 2024a).

Hazard assessments are also conducted on a country-wide scale. In Germany, for example, stationary IDF values are provided by the aggregated rainfall hazard dataset (KOSTRA-DWD). This dataset is widely recognized in engineering practice as a standard for assessing extreme events, particularly in applications such as urban drainage planning and flood risk modeling (Hundhausen et al., 2024). KOSTRA-DWD is derived from interpolated station data, which results in relatively low spatial resolution and, consequently, smoothed patterns of precipitation extremes. In contrast, the radar-based high-resolution precipitation climatology (RADKLIM) product offers very fine spatial resolution (1 km), but despite adjustments using in-situ observations, RADKLIM tends to underestimate extreme precipitation intensities when compared to direct ground-based observations (Pöschmann et al., 2021; Lengfeld and Marra, 2024). Additionally, CPM simulations from the KLIWA project ('Climate Change and Consequences for Water Management', www.kliwa.de) are available, but they are limited in domain size to southern Germany (Hundhausen et al., 2023, 2024).

Existing precipitation records are unlikely to provide accurate estimates of the magnitude and frequency of short-duration precipitation extremes under climate change. These are usually limited by (i) sufficiently dense and sub-daily precipitation data (Hundhausen et al., 2024; Dallan et al., 2022; Prein et al., 2017; Sun et al., 2021; Hundhausen et al., 2024; Poschlod, 2021); and (ii) statistical methods that allow us to extrapolate extreme precipitation return levels under limited data availability and non-stationary conditions (Laux et al., 2023; Dallan et al., 2024a). Moreover, process-based hydraulic projections for pluvial floods in urban catchments based on realistic precipitation design levels under future climate conditions are missing today in most countries worldwide.

Here, we overcome these limitations through the utilization of kilometer-scale hourly precipitation (RADKLIM) and high-resolution daily temperature (gridded hydrometeorological data, HYRAS) data, and the implementation of a novel CPM ensemble for the whole of Germany. To assess changes in hourly precipitation extremes, we apply the TENAX model. This new approach integrates daily temperature as a covariate, aligning with observed scaling rates, which makes it a suitable candidate for risk assessment under non-stationary climate conditions. By adhering to this physically consistent approach, we project the impact of future climate conditions on pluvial flood risk at the commune level through high-resolution and process-based hydrodynamic modeling (Ochoa-Rodriguez et al., 2015; Westra et al., 2014).

We hypothesize that the future intensification of precipitation extremes will result in higher inundation levels, severely affecting Germany's infrastructure compared to today. As a German-wide assessment of inundation levels is not feasible with a computationally demanding and detailed modeling approach, we selected two typical communes in southern Germany. This study illuminates the potential impacts of different warming scenarios in two German municipalities. The provided hourly precipitation design values can be used to assess localized climate risks in urban catchments across Germany. Moreover, the methodological approach may serve as a blueprint for other countries and regions across Europe with similar climate change signals and data infrastructures.

2. Study region & Methods

The study focuses on Germany, where non-stationary, kilometer-scale extreme hourly precipitation values are derived. Hydrodynamic modeling is conducted in the Oberland region of southern Bavaria — an area recognized as a hot spot for extreme convective precipitation events (Laux et al., 2023). As a result, the derived precipitation design values rank among the highest in the country, making this region particularly suitable for investigating the impacts of climate change on pluvial flood risk. The hydrodynamic simulations are carried out in two municipalities: Garmisch-Partenkirchen and Weilheim.

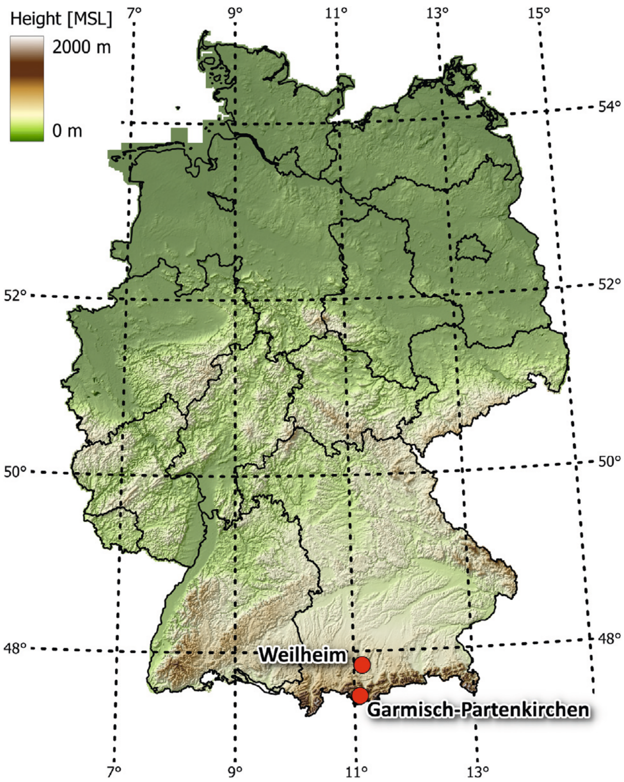

Fig. 1. Digital Elevation Model (DEM) for Germany. The locations of the two municipalities for the hydrodynamic modeling, i.e., Weilheim and Garmisch-Partenkirchen, in southern Germany are highlighted.

Garmisch-Partenkirchen, located in the alpine region, features complex topography. The elevation ranges between 671 and 1984 m a.s.l. altitude, which necessitates high-resolution modeling to resolve surface flow paths. In contrast, Weilheim lies in the alpine foreland, with less steep terrain but different hydrological and infrastructural characteristics. Here, the elevation ranges between 544 and 667 m a.s.l. altitude. Fig. 1 illustrates the location and topography of both municipalities within Germany. Due to distinct differences in elevation, land use, and sewer system configuration, each site requires a tailored hydrodynamic modeling approach (see Section 2.2.1).

The methodology comprises a climate hydrodynamic modeling chain (CHMC), as illustrated in Fig. 2. Following are the four main steps as well as methodological details:

1. Apply the TENAX model (Section 2.1) with the RADKLIM (Section 2.3.1) and the spatially refined HYRAS (Section 2.3.2) data (i.e., RADKLIM grid) to derive stationary hourly precipitation intensities at a 100-year return level.
2. Repeat step 1, using the climate change signals (ΔT, $\sigma_{future}/\sigma_{past}$, n_{future}/n_{past}) from the NUKLEUS CPM ensemble (Section 2.4) to estimate non-stationary return levels of precipitation extremes.
3. Assess the difference of non-stationary future precipitation return levels $P_{RL}^{Future,NS}$ (i.e., precipitation return levels obtained from TENAX for the future $P_{RL}^{TENAX,f}$ minus present TENAX return levels $P_{RL}^{TENAX,p}$) and impress them onto the present stationary KOSTRA-DWD return levels $P_{RL}^{KOSTRA,p}$ to correct for systematic magnitude deviations (referred to as RL bias correction) between ground observations and radar data:

$$P_{RL}^{Future,NS} = P_{RL}^{KOSTRA,p} + (P_{RL}^{TENAX,f} - P_{RL}^{TENAX,p}). \tag{1}$$

4. Perform hydrodynamic modeling and derive flood risks in the two selected municipalities based on stationary ($P_{RL}^{KOSTRA,p}$) and non-stationary ($P_{RL}^{Future,NS}$) return levels (Section 2.2.1).

2.1. Computing hourly extreme precipitation return levels

The TENAX (TEmperature-dependent Non-Asymptotic statistical model for eXtreme return levels) model (Marra et al., 2024) is a framework to compute extreme precipitation return levels for present and future climates by incorporating temperature as a covariate in a physically consistent manner; i.e., by preserving the observed thermodynamic link between air temperature and short-duration extreme precipitation intensities (Fowler et al., 2021b). Essentially, the concept is to distinguish extreme precipitation from the occurrence of precipitation events at a particular temperature. In contrast to the classical extreme value theory, the model is based on non-asymptotic statistics, which means that extremes are samples from independent realizations of the process of interest, known as "ordinary events". In this way, the stochastic sampling of both temperature and precipitation severity, inherent in natural processes, is preserved. These approaches were shown to provide estimates of extreme return levels as high as 100 years with largely reduced uncertainty compared to traditional methods (Zorzetto et al., 2016; Marra et al., 2019). For example, Dallan et al. (2024a) showed that estimates from 10 years of CPM simulations based on the SMEV method are comparable to traditional GEV estimates used with (i) three values in each year together with (ii) a prior distribution to limit the estimation uncertainty of the shape parameter. TENAX requires minimal input data: (i) observed time series of precipitation (at the same temporal resolution as that required to estimate precipitation return levels) and temperature (T_p, with a daily temporal resolution at least) representing the present climate; (ii) information from climate models on the change in mean and standard deviation of temperature during wet days ($\Delta T = T_f - T_p$ and $\frac{\sigma_f}{\sigma_p}$, respectively); and (iii) details of the change in the total annual number of precipitation events ($\frac{n_f}{n_p}$).

TENAX is composed of three components: (i) a "magnitude component" — a non-stationary statistical model for the cumulative distribution function of the magnitude of precipitation events, in which temperature is included as a covariate; (ii) a "temperature component" — a probability density function of temperatures during precipitation events; and (iii) a "return level estimation component". The TENAX model hinges on the assumption that temperature is the covariate that describes most of the variability in extreme precipitation at the scale of interest and that the dependence of extreme precipitation on this covariate (i.e., the magnitude model below) is invariant in time. The model components are briefly summarized below; for more details regarding the conceptualization and parameterization of the model, physical robustness, sensitivity, and validation tests, please refer to Marra et al. (2024).

2.1.1. Magnitude component

Precipitation magnitudes x for a duration t_D of interest are defined as the maximum intensities at the duration t_D observed during independent precipitation events (for more information on their identification refer to Marra et al. (2020)). Precipitation magnitudes (x) are modeled using the Weibull distribution, in which scale and shape parameters depend explicitly on near-surface air temperature (T):

$$W(x;T) = 1 - e^{-\left[\frac{x}{\lambda_0 \cdot e^{aT}}\right]^{\kappa_0 + bT}}, \tag{2}$$

where λ_0 and a describe the exponential dependence of the scale parameter on temperature similar to the one used in extreme precipitation-temperature scaling relations, and κ_0 and b describe the linear dependence (if exists) of the shape parameter on temperature.

2.1.2. Temperature component

The temperature during wet days is defined as the average temperature during the 24 h preceding the peak intensity of the precipitation

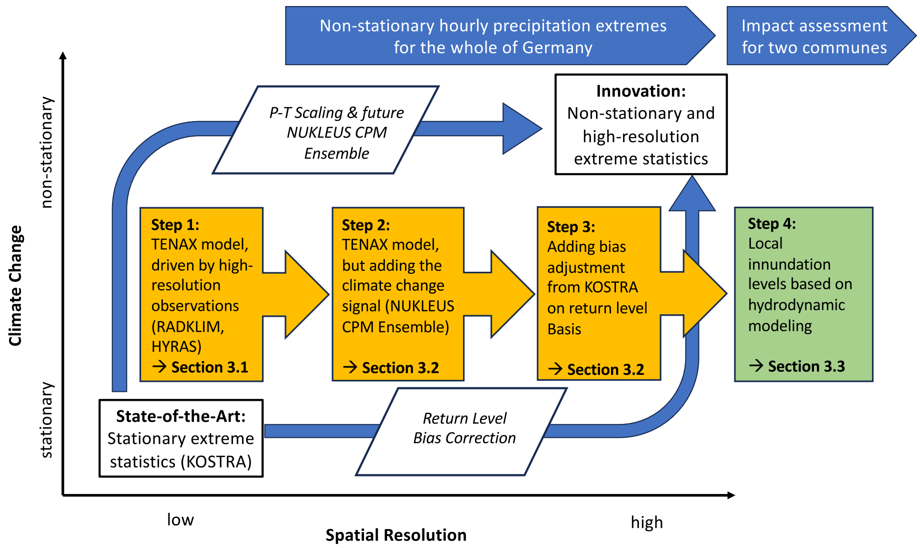

Fig. 2. Schematic overview illustrating the four main methodological steps (Section 2). Steps 1–3 comprise how to derive the new non-stationary precipitation statistics for Germany, and step 4 is the application of these data for 2 municipalities in the pre-alpine Bavarian region (southern Germany).

event. It is modeled using a Generalized Gaussian distribution with a shape parameter equal to 4. Its probability density function is:

$$g(T) = \frac{2}{\sigma \cdot \Gamma(1/4)} \cdot \exp\left[-\left(\frac{T-\mu}{\sigma}\right)^4\right], \tag{3}$$

where μ is the location and σ is the scale parameters. For additional details about this choice and the possible physical reasoning behind it, refer to Marra et al. (2024).

2.1.3. Return level estimation component

Ordinary statistics show that when the marginal CDF $F(x)$ describing all the independent realizations of the process of interest is known, the CDF $G(x)$ of annual maxima emerging from a finite number n of independent events per year sampled from $F(x)$ can be written as:

$$G(x) = F(x)^n. \tag{4}$$

Having determined the magnitude $W(x;T)$ and the temperature $g(T)$ components, T_i can be stochastically generated with $i = 1, \dots, N$ sampled from $g(T)$ to produce a Monte Carlo representation of $F(x)$. It is then possible to estimate the distribution of annual maxima using the Simplified Metastatistical Extreme Value (SMEV) formulation (Marra et al., 2019):

$$G_{\mathrm{TENAX}}(x) = \left(\int_D W(x;T) \cdot g(T) dT\right)^n \simeq \left(\frac{1}{N}\sum_{i=1}^{N} W(x;T_i)\right)^n, \tag{5}$$

where D is the domain of the temperature model, N is the number of stochastically generated events, and n is the average number of independent events in a year. Precipitation return levels can then be computed by the inversion of Eq. (5).

2.2. Flood risk assessment

2.2.1. Hydrodynamic modeling

Hydrodynamic modeling was performed in two municipalities using two different model approaches. For Weilheim, the rainwater drainage system plays an important role during heavy precipitation events. There, streams originating from the outlying regions are transported to the urban sewer system, where they interact with the drainage of residential areas. To accurately model the flow processes and feedback of the surface and the rainwater drainage system, the 2D surface model HydroAS (Hydrotec, 2023) is bi-directionally coupled with the 1D sewer network model Hystem-Extran (more information following https://itwh.de/en/). This framework allows for the parallel calculation of all relevant flow processes on and under the surface and, therefore, for realistic flood risk mapping. In Garmisch-Partenkirchen, the storm water drainage system is fragmented and not part of a larger network. Instead, there are several single pipes connecting sealed areas such as parking lots to the nearest river. These pipes can be modeled directly in the hydrodynamic model using so-called 1D culvert boundary conditions, which connect two points of the computational mesh over a larger distance. In this case, this method reduces the modeling effort significantly compared to the full coupling of the 2D surface model with a 1D storm water model while achieving the same accuracy. Here, the H_SIM-2D model is applied, allowing for higher resolution at feasible simulation times. Due to the size of the catchment area relevant for pluvial flooding, the model domains cover a region of 60 km^2 for Garmisch-Partenkirchen and 30 km^2 for Weilheim, respectively. Data about sewer networks are provided by the local Municipal Building Authorities.

Both hydrodynamic 2D models are based on shallow-water equations and use an irregular mesh of triangles and quadrilaterals for flexible terrain adaptation. They assume hydrostatic pressure and integrate the Reynolds-averaged Navier–Stokes equations (Pironneau, 1988; Tan, 1992). The hourly precipitation rate is applied as a design storm with a center-weighted distribution according to DVWK (1999), using three different rain intensities, with the middle intensity being the highest. At each node of the computational mesh, an individual effective precipitation amount is defined and calculated with the SCS Curve Number Loss Model (USDA National Resources Conservation Service, 2004). This method considers the impact of land use, soil properties, soil moisture, and rain intensity on the infiltration rate. Both models use a newly developed depth-dependent roughness approach for shallow surface runoff (Feldmann et al., 2023).

2.2.2. Hazard and risk assessment

Following the simplified method for hazard and risk assessment (LfU, 2017), the results of hazard identification are supported by identifying objects (e.g., buildings) affected by or at risk of pluvial flooding. This is a robust method when detailed data on each building is not available. The susceptibility to flooding is determined by intersecting the objects with the identified flood areas (from hazard identification of Section 2.2.1). The objects are marked according to their susceptibility to flooding, as classified in Table 1, based on a simulated extreme hourly precipitation event of a 100-year return period. This procedure

Table 1
Flood risk categories following (LfU-Bayern, 2022).

Category	Flood risk	Water level [cm]
0	No risk	0
1	Low	5–10
2	Moderate	10–50
3	High	50–100
4	Very high	>100

Table 2
Mean annual 2 m air temperature bias (°C) of the NUKLEUS CPMs used in this study for the period 1961–1990.

CPM	Oberland region	Germany
CCLM EC-Earth3-Veg	+0.29 °C	+0.32 °C
CCLM MIROC6	+0.25 °C	–0.07 °C
ICON-CLM EC-Earth3-Veg	+0.39 °C	+0.11 °C
ICON-CLM MPI-ESM-HR	+0.50 °C	+0.24 °C

is done for current climate conditions (KOSTRA-DWD) and two changing climate scenarios applying the NUKLEUS +2 °C and +3 °C CPM ensemble mean. Relative changes [in %] between current and future climate conditions are calculated.

2.3. Observed data

2.3.1. Precipitation

Hourly gridded precipitation data for the period 2001–2020 for Germany were obtained from the radar-based high-resolution precipitation climatology product (RADKLIM, Version 2017.002) of the German Weather Service (DWD) (Winterrath et al., 2018). The hourly precipitation sums ("RW product") result from the radar-based precipitation estimation (RADOLAN) that are adjusted with precipitation measurements by gauges. The data are available on a 1 km × 1 km grid in a polar stereographic projection. The data set is quality-controlled, including climatological correction methods of clutter- and signal reduction with height and distance caused by different effects like overshooting, attenuation, and increase of the measurement volume and spokes. The data set is freely available and will be extended annually.

Gridded data of hourly precipitation return periods (design precipitation) over Germany were obtained from the KOSTRA-DWD product (Version 2020 Junghänel et al., 2017). This data is considered state-of-the-art in engineering for sizing water management infrastructure such as sewer networks, pumping stations, and retention basins. They are commonly employed for designing urban drainage and infiltration systems. KOSTRA-DWD is utilized as the stationary (present-climate) precipitation return level estimate $P_{RL}^{KOSTRA,p}$.

2.3.2. Temperature

Daily gridded (5 km × 5 km) temperature data T_p spanning the period 2001–2020 were derived from the HYRAS-DE-TAS (Version v5.0) product. These observational datasets (HYRAS) are compiled from measurements collected within Germany and its neighboring countries, utilizing approximately 1300 stations for interpolation. More technical information can be found in Razafimaharo et al. (2020).

2.4. Climate model data

The project NUKLEUS (German acronym for Useable Local Climate Information for Germany) generated an ensemble from regional (high-resolution) downscaling of three Global Circulation Models (GCMs), obtained from the CMIP6 ensemble — namely EC-Earth3-Veg, MPI-ESM-HR, and MIROC6 (Table 3). To ensure a representative selection of global climate models (GCMs) for downscaling, the project relied on the EURO-CORDEX GCM selection framework (Sobolowski et al., 2023), which identified six CMIP6 GCMs as particularly suitable for regional climate modeling over Europe. This selection was based on model performance metrics and the ability to capture the plausible range of climate sensitivity. From this set, three GCMs were chosen to span the low (MIROC6), medium (MPI-ESM-HR), and high (EC-Earth3-Veg) ends of climate sensitivity. This subset was selected by the NUKLEUS project team to ensure that the ensemble captures a broad range of potential future climate responses consistent with the CMIP6 framework. To retain the large-scale consistency with the driving GCMs and to ensure numerical stability (Warner, 2011), the downscaling is performed using two nesting steps: First, to the EURO-CORDEX domain with a resolution of 12.5 km and then further down to 3 km in a convection-permitting mode for a domain covering Germany and its surroundings (Fig. 4). The simulations for the coarse-scale European domain were performed transiently, using the historical experiments from 1951–2014, followed by the ssp370 scenario (2015–2099). For all experiments, the first GCM realization (r1i1p1f1) was applied. The 3 km and 1 h-resolution CPM simulations span time slices of 30 years, with a historical period from 1961–1990 and two scenario periods covering the Global Warming Levels (GWL) +2 °C and +3 °C compared to pre-industrial conditions (Table 3). In this study, the GWL approach is followed as it focuses on the level of warming, which is more relevant for the assessment of the impact of climate change and user applications, for example, extreme precipitation and heat stress, than the specific path to that warming. This reduces uncertainty in climate projections and provides comparable results across different emission scenarios, supporting better policy framing and adaptation measures. The +2 °C and +3 °C GWLs are considered reasonable because they align with the key temperature thresholds set by the Paris Agreement and current climate projections. The +2 °C scenario represents a moderate warming level for near-term adaptation, while the +3 °C scenario reflects a stronger warming with longer-term impacts, both of which are relevant for designing effective climate adaptation measures. The recent occurrence of 12 consecutive months with global mean surface temperatures at or above 1.5 °C above preindustrial levels suggests that the world may have already crossed the long-term 1.5 °C warming threshold set by the Paris Agreement earlier than expected (Cannon, 2025), and it is expected that current policies will lead to an approximate warming of 3 °C until the end of the century (United Nations Environment Programme, 2024).

The GWLs were calculated following Teichmann et al. (2018). As we apply the period 1961–1990 in our analysis as a reference rather than a preindustrial time slice, it must be considered that the historical reference period has a GWL of +0.42 °C (compared to preindustrial time). Here, data from four NUKLEUS GCM-RCM model combinations (Table 3) are used, based on two RCMs: first, the ICON-CLM (Van Pham et al., 2021) in version 2.6.5-rc is grounded on the icosahedral modeling framework ICON (Zängl et al., 2015). CCLM (COSMO-CLM, Sørland et al. (2021)) is applied in its final version COSMO6. For both RCMs, the parameterization for deep convection is switched off at the 3 km resolution, providing CPM ensembles for the whole of Germany. Since air temperature is used directly as a covariate in the TENAX model, we validated the annual mean temperature bias of the CPM simulations with respect to station observations. Table 2 summarizes the spatially averaged biases for the Bavarian Oberland region and Germany.

In the Bavarian Oberland region, where the TENAX model is applied, biases range between +0.25 °C (CCLM-MIROC6) and +0.50 °C (ICON-CLM MPI-ESM-HR). These values are slightly higher than the national averages but still lie within acceptable bounds for regional climate applications.

The seasonal cycle of monthly mean temperature and precipitation biases in the Oberland region is shown in Figure S1(a), demonstrating that the CPM ensemble captures temperature well throughout the year. Monthly biases remain within ±1 K for most months, in which convective events prevail. Although not used for the non-stationary TENAX model, the precipitation bias is shown in Figure S1(b). Biases

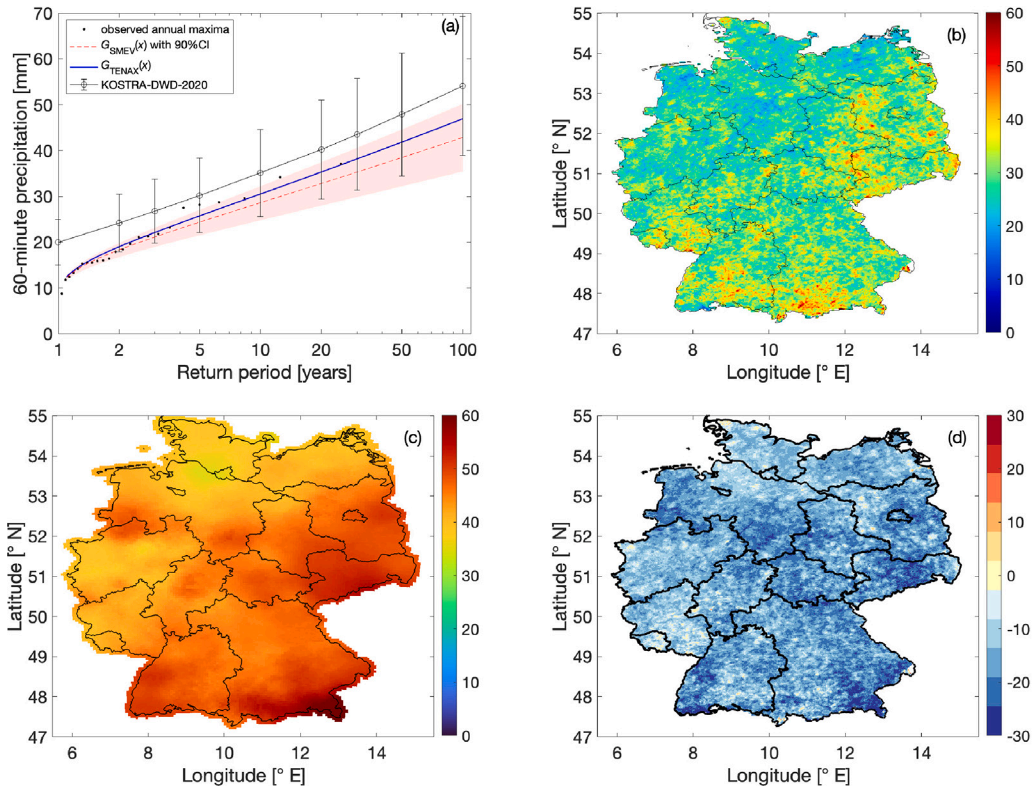

Fig. 3. Hourly precipitation values for a 100-year level [mm] using RADKLIM and HYRAS data (a) at Garmisch-Partenkirchen (Fig. 1) based on the TENAX model, the SMEV model, and KOSTRA-DWD (Version 2020). (b) TENAX hourly precipitation values for a 100-year level [mm] for the whole of Germany. (c) shows the corresponding precipitation extremes based on the KOSTRA-DWD [mm] as a reference. (d) shows the deviations [mm] between the TENAX and KOSTRA-DWD.

Table 3
The NUKLEUS CPM ensemble, driven by CMIP6 simulations applied as initial and boundary conditions. For each GCM, the r1i1p1f1 realization was used for the historical and ssp370 scenario. The period to achieve Global Warming Levels (GWL) of +2 °C and +3 °C using the ssp370 scenario is shown for each GCM.

GCM	Reference (historical) (ssp370)	RCMs	GWL +2 °C period	GWL +3 °C period
EC-Earth3-Veg	EC-Earth-Consortium (2019a)	ICON-		
		CLM		
	EC-Earth-Consortium (2019b)	CCLM	2024–2053	2047–2076
MPI-ESM-HR	Jungclaus et al. (2019)	ICON-		
		CLM		
	Schupfner et al. (2019)		2037–2066	2066–2095
MIROC6	Tatebe and Watanabe (2018)	CCLM		
	Shiogama et al. (2019)		2038–2067	2070–2099

in the Oberland region tend to be higher than in Germany (Figure S2). Moreover, we analyzed the representation of extreme precipitation by comparing the IDF curves of the 100-year return level for the four CPM simulations with KOSTRA-DWD, exemplarily shown for Weilheim (Figure S3). The CPMs are shown to most often lie within the uncertainty range of the KOSTRA-DWD data, indicating that sub-daily extreme precipitation events can be well represented in the CPM ensemble.

Due to different projections and spatial resolutions, observed and modeled data are regridded onto a regular lon/lat grid of 0.01° (approx. 1 km) by applying the nearest neighbor interpolation. Since the primary goal is to preserve extreme values accurately, the nearest neighbor interpolation is used. To assess the impact of different interpolation (regridding) strategies within the hydrometeorological modeling chain, we compared three well-established approaches (i.e., bilinear, bicubic, distance-weighted) against the nearest neighbor method using the 99th percentile of precipitation extremes at station Garmisch-Partenkirchen under the +3 °C GWL scenario (EC-Earth3-Veg – CCLM). The differences between the methods remained below 1%, indicating that regridding contributes only marginally to the overall uncertainty of the hydrodynamic modeling.

3. Results

3.1. Extreme precipitation values under current climate conditions

The TENAX-derived return levels of hourly precipitation values based on RADKLIM and HYRAS for Garmisch-Partenkirchen are shown in Fig. 3a. It can be demonstrated that TENAX provides a good fit to the RADKLIM data and closely follows benchmark stationary models, such as the SMEV (see method Section 2.1), and the empirical annual maxima. It, however, deviates in magnitude due to the fundamentally different measurement principle between radar-based precipitation estimation and ground-based observations, as also found by Lengfeld and Marra (2024). We evaluated the goodness of the TENAX model in representing extreme precipitation intensities under changing climate conditions by checking the scaling rates (Figure S4). It is demonstrated that the TENAX-derived precipitation-temperature scaling rates are in close correspondence to the observed scaling rates and that the values are within expected ranges and higher than the C–C scaling rates. As can be expected for short-term convective events, the spatial patterns do not distinctly align with the topographic conditions of Germany (Lengfeld et al., 2019).

For the whole of Germany, there is an NW-SE gradient of increasing precipitation extremes for the TENEAX model (Fig. 3b) and the corresponding precipitation extremes of the state-of-the-art KOSTRA-DWD

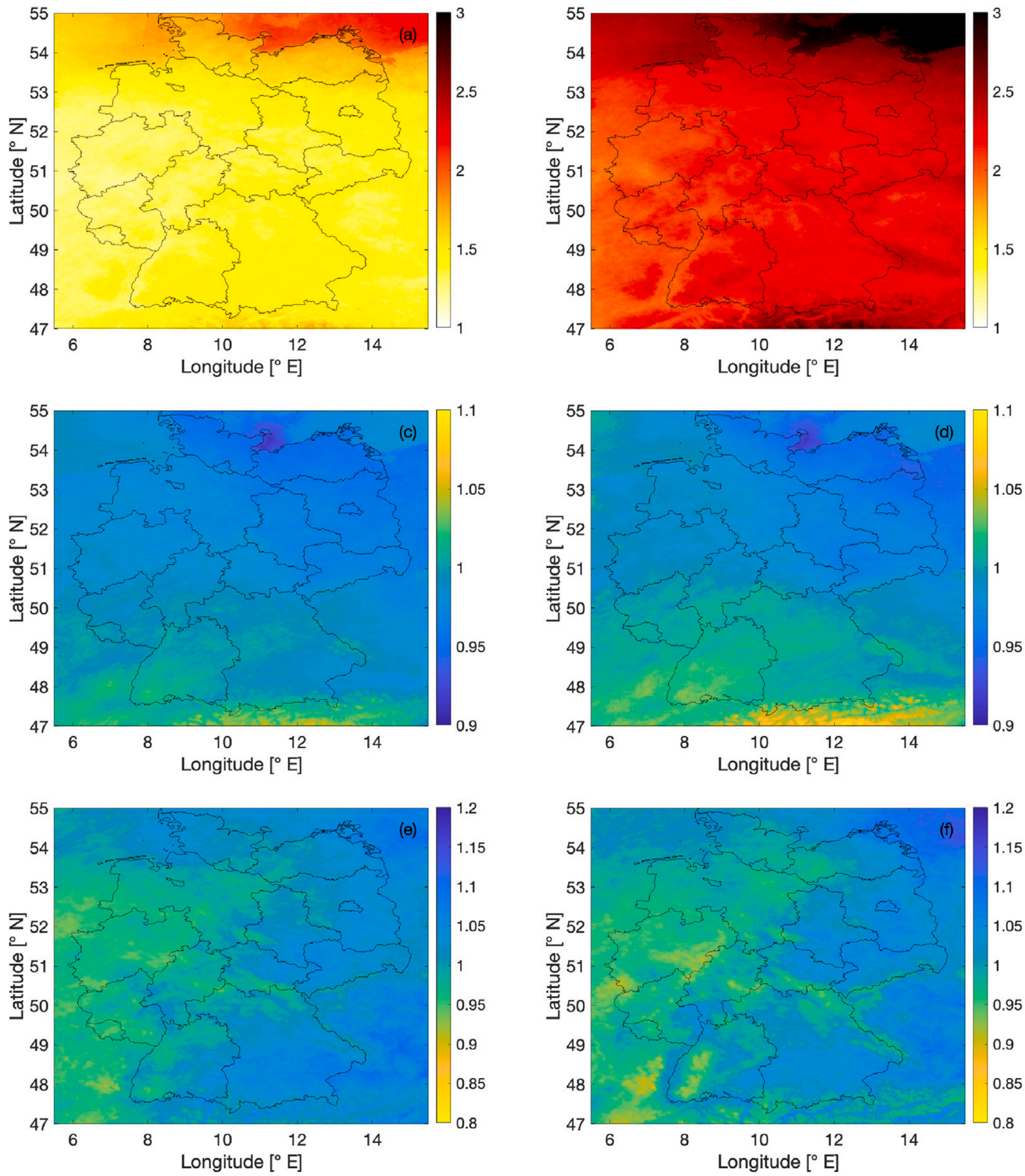

Fig. 4. NUKLEUS +2 °C CPM ensemble mean of (a) mean air temperature increase [°C] compared to the reference period 1961–1990 with a GWL of +0.42 °C, (c) change (factor) of the standard deviation of air temperature [-], and (e) change (factor) of the occurrence of precipitation events. NUKLEUS +3 °C GWL CPM ensemble shown in (b), (d), and (f).

product (Fig. 3c). The TENAX-derived hourly precipitation extremes are notably more heterogeneous than those derived from KOSTRA-DWD, as the latter are interpolated from stations while TENAX is here applied to weather radar data, from which they inherit some spatial noise (e.g., see Lengfeld and Marra, 2024), though local spatial clustering of high precipitation values corresponds well between the two methods. From visual inspection, heavy precipitation events are less influenced by orography compared to KOSTRA-DWD (see Fig. 1 as a reference). Fig. 3d depicts the deviation in the magnitude between TENAX and KOSTRA-DWD. TENAX, on spatial average for the 100-year return level, is approximately 15.4 mm h^{-1} lower compared to KOSTRA-DWD (with a standard deviation of 0.8 mm h^{-1}). This deviation needs consideration to model extreme precipitation values under a non-stationary climate, i.e., future climate conditions.

3.2. Extreme precipitation values under future climate conditions

To derive the expected climate signal for the future, the NUKLEUS CPM ensemble (see Section 2.4) is analyzed for two scenarios, following a +2 °C and a +3 °C global warming levels (GWL) compared to the preindustrial conditions. Fig. 4 illustrates the NUKLEUS CPM ensemble mean of mean air temperature increase, the change (factor) of the standard deviation of air temperature, and the change (factor) of the average annual number of precipitation events under both scenarios, compared to the historical reference period (1961–1990). The historical reference period has a GWL of 0.42 °C compared to preindustrial times. Since the regional mean air temperature increases across the entire domain are approximately +1.75 °C for the +2 °C and +2.9 °C for the +3 °C GWL scenario (Fig. 4a,b), the regional air temperature signals are therefore slightly higher than the averaged global air temperature signals. For both scenarios, the change factors of the standard deviation of the mean air temperature follow a north-south gradient, with a higher change factor (>1) in the north and values around 1 and higher in the south. Topographic effects are visible, as the Alpine regions at the southern border of the domain reach the highest change factors (up to 1.1). This effect is more pronounced for the +3 °C scenario, whereas the patterns correspond well between the scenarios (Fig. 4c,d). The air temperature variability within the ensemble, expressed as the coefficient of variation, is comparatively higher for the +2 °C compared to the +3 °C scenario (Figure S5). This indicates a relatively higher

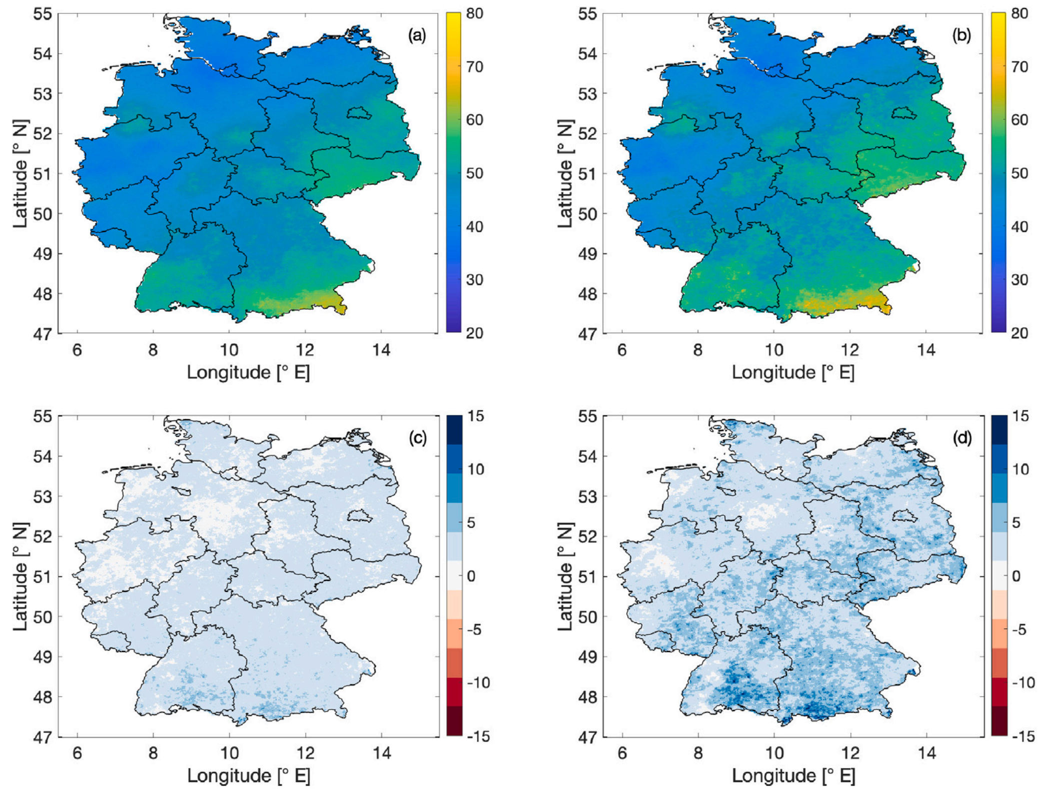

Fig. 5. Adjusted non-stationary hourly extreme precipitation intensities [mm] for a 100-year return level under the GLW +2 °C (a) and +3 °C (b) scenarios. Differences in precipitation intensities compared to the KOSTRA-DWD (i.e., stationary assessment) for the +2 °C (c) and the +3 °C (d) GLW scenario.

inter-model ensemble uncertainty for the lower warming rate. In terms of change in the occurrence of precipitation events (Fig. 4e,f), there is a west-east gradient towards increasing events in the eastern parts of Germany, and comparatively fewer events are expected under the +3 °C scenario in western Germany. Exploring the impact of these changes on extreme precipitation return levels using the TENAX model, a higher impact can be expected from the temperature change compared to the change in precipitation occurrence, as visible in the sensitivity experiments conducted for Garmisch-Partenkirchen (Figure S6).

The newly non-stationary hourly extreme precipitation intensities for a 100-year event are illustrated in Fig. 5 for both scenarios. They are derived using the TENAX model based on the NUKLEUS CPM ensemble statistics and KOSTRA-DWD to adjust the magnitude (see Eq. (1) in Section 2). Overall, in both scenarios, the patterns of the stationary KOSTRA-DWD approach are reproduced but provide moderately more spatial details (Fig. 5a,b). Local increases up to 20 mm h^{-1} compared to the historical intensities of KOSTRA-DWD can be found (Fig. 5c,d). The spatial average of the increase amounts to approximately 2.1 mm h^{-1} (standard deviation of 0.18) and 3.7 mm h^{-1} (standard deviation of 0.35) under the GLW +2 °C and the GLW +3 °C scenario, respectively. Local differences up to 20 mm h^{-1} can be observed under the GLW +3 °C scenario, particularly in Baden-Wuerttemberg and Bavaria, in southern Germany, where our two study cases are located.

3.3. Impacts of climate change on local flood risk

We conducted 3 hydrodynamic simulations, one based on the extreme precipitation intensities of KOSTRA-DWD, one for the +2 °C, and another for the +3 °C GWL scenarios. The simulations were applied for the two municipalities Garmisch-Partenkirchen and Weilheim, in slightly different model settings (see Section 2.2.1). The resulting differences in inundation levels emerging from the two GWL scenarios relative to the stationary KOSTRA-DWD input are calculated and illustrated in Figs. 6 and 7 for Garmisch-Partenkirchen and Weilheim, respectively.

Identifying buildings at risk of pluvial flooding, we finally derive the summary statistics of relative changes for both municipalities (Fig. 8). The different classes refer to flood risk categories that correspond to water level ranges (Table 1).

For Garmisch-Partenkirchen (Fig. 8a), the number of buildings is decreasing for the no-risk category (up to −7.1% and −9.2% for the +2 °C and the +3 °C GWL scenarios, respectively), and increasing considerably for the high-, and very high-risk categories, in the latter case, up to +19.9% and +24.6% for the +2 °C GWL and the +3 °C GWL scenario, respectively. While the pattern of changes is similar for both future scenarios for Garmisch-Partenkirchen, this is not the case for Weilheim (Fig. 8b), where both GWL scenarios deviate remarkably. The relative changes in the number of affected buildings are increasing exceptionally for the +3 °C GWL scenario (up to +40.6% and +60.0% for the high- and the very high-risk category), the changes are highest for category 3 (high-risk, up to +20.8%) and is as small as +10.0% in the very high-risk category for the +2 °C GWL scenario.

Figs. 9 and 10 show the flow intensity, which is the product of flow velocity and water depth, driven by the different precipitation scenarios compared to KOSTRA-DWD 2020. In Garmisch-Partenkirchen, the flow intensities are relatively high because of the high elevation gradients (steep terrain). In contrast, Weilheim experiences high flow velocities only along watercourses; the rest of the terrain is mostly flat. As a result, water tends to accumulate in low-lying areas and depressions, which can still pose a threat to buildings. This explains why there is little to no increase in flow intensities in Weilheim under the +2 °C GWL scenario.

4. Discussion

To build future climate-proof water systems and reduce the risk of critical infrastructure, short-duration extreme precipitation design

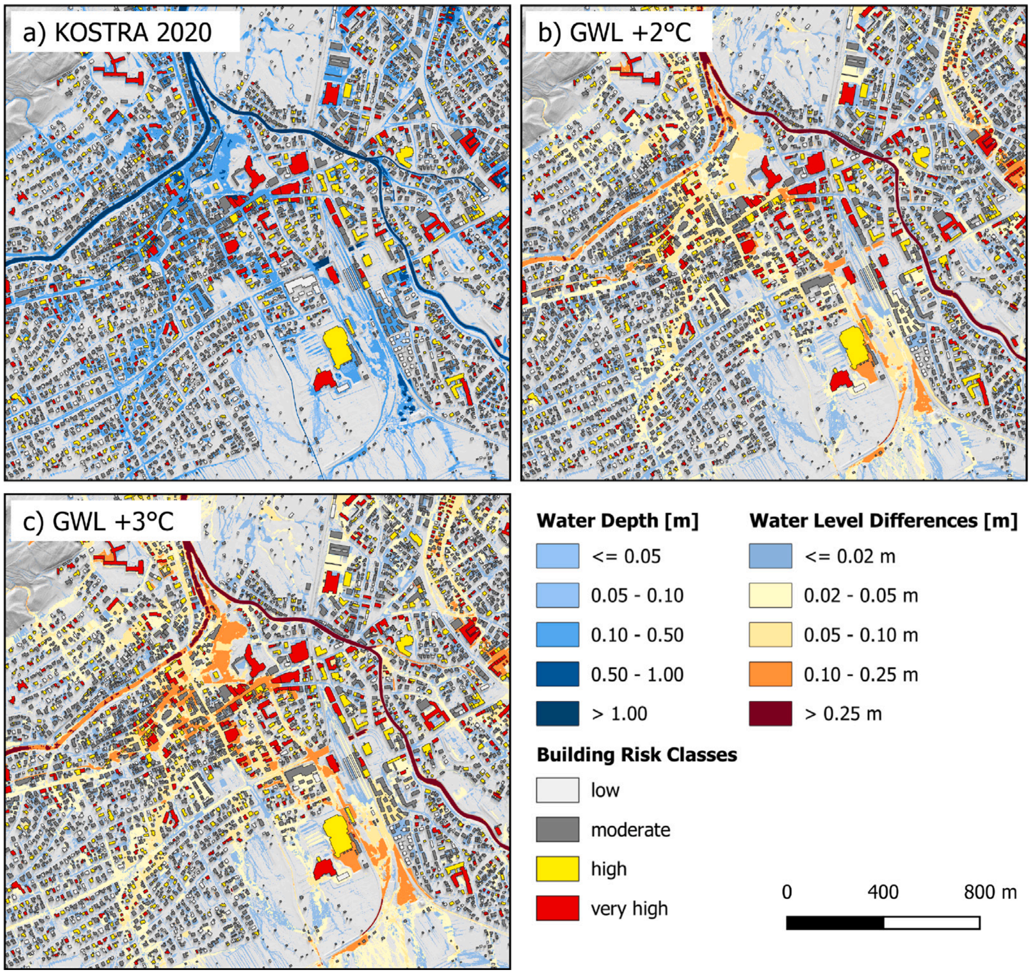

Fig. 6. Inundation areas, illustrated as water depth [m] in Garmisch-Partenkirchen calculated with the hydrodynamic model, driven by different precipitation scenarios, KOSTRA-DWD Version 2020 (a), GWL +2 °C (b) and GWL +3 °C (b). Figures b and c illustrate the water level differences [m] to the KOSTRA-DWD simulation (a). Furthermore, the individual flood risk of buildings is depicted. The Figure shows only a subset of the model domain.

storms must be updated (Hosseinzadehtalaei et al., 2020). Our research has therefore delved into the assessment of future hourly precipitation extremes based on the new statistical model TENAX (Marra et al., 2024) and high-resolution observational and RCM data for the whole of Germany (i.e., RADKLIM, HYRAS, and NUKLEUS CPM). We derived hourly precipitation extremes for Germany for +2 °C and +3 °C GWL scenarios and assessed the corresponding hydrodynamical impact for two representative communes in the Bavarian Oberland region (southern Germany).

The correspondence between the modeled and observed extreme precipitation patterns (Fig. 3) underscores the utility of RADKLIM data in capturing the spatial distribution of precipitation extremes. However, our comparison with KOSTRA-DWD data also revealed notable differences. While the greater scatter using RADKLIM is plausible due to its higher actual resolution (compared to the spatially interpolated KOSTRA-DWD product), significant deviations in the magnitude highlight challenges in relying solely on the RADKLIM and HYRAS products for the estimation of extreme precipitation events (Pöschmann et al., 2021). Deviations from the KOSTRA-DWD-derived precipitation extremes are due to the fundamental differences in the measurement principle of radar estimations (direct point measurement of stations versus indirect estimates from a large atmospheric volume of radar) as well as the limited length of the radar precipitation estimates (20 years only) (Ochoa-Rodriguez et al., 2015; Lengfeld et al., 2020). For this purpose, a magnitude adjustment ("bias" correction on return level basis) of the kilometer-scale TENAX simulations based on RADKLIM has been performed (Fig. 5), which reflects both the magnitude of the KOSTRA-DWD product as well as the impact of climate change. While complex bias correction methods on the raw precipitation values may introduce additional uncertainties (Laux et al., 2021), the applied delta approach may suffice given the relatively short observational period (Shrestha et al., 2017; Dang et al., 2017). As expected, (convective) precipitation extremes of short durations do not show strong relations with topography (Ban et al., 2015) as represented in KOSTRA-DWD, and are rather uniformly distributed over Germany (Winterrath et al., 2019). The obtained scaling rates for 1-h extremes are in agreement with observed scaling rates across Europe (Bürger and Bronstert, 2014; Marra et al., 2024; Dallan et al., 2022; Persiano et al., 2020), further supporting the potential of RADKLIM and HYRAS as a surrogate dataset for applications with scarce observation station data or regional-scale assessments of extreme precipitation events across Germany.

For risk assessment of future extreme events, high-resolution CPM ensemble simulations from a CPM ensemble are used as input for the TENAX model. By using the new NUKLEUS CPM ensemble, it could be demonstrated that changes in the ensemble mean vary remarkably amongst the 2 °C and the 3 °C GWL scenarios (Fig. 4). Based on the NUKLEUS CPM ensemble statistics, future hourly extreme precipitation intensities are derived in unprecedentedly high spatial detail. The resulting difference in the hourly extreme precipitation intensities between the present and future climates can vary locally up to 15% across Germany. Dallan et al. (2024b) found an average increase of 30% in the 100-year return level over the Greater Alpine-Mediterranean region for the end of the century using the SMEV approach.

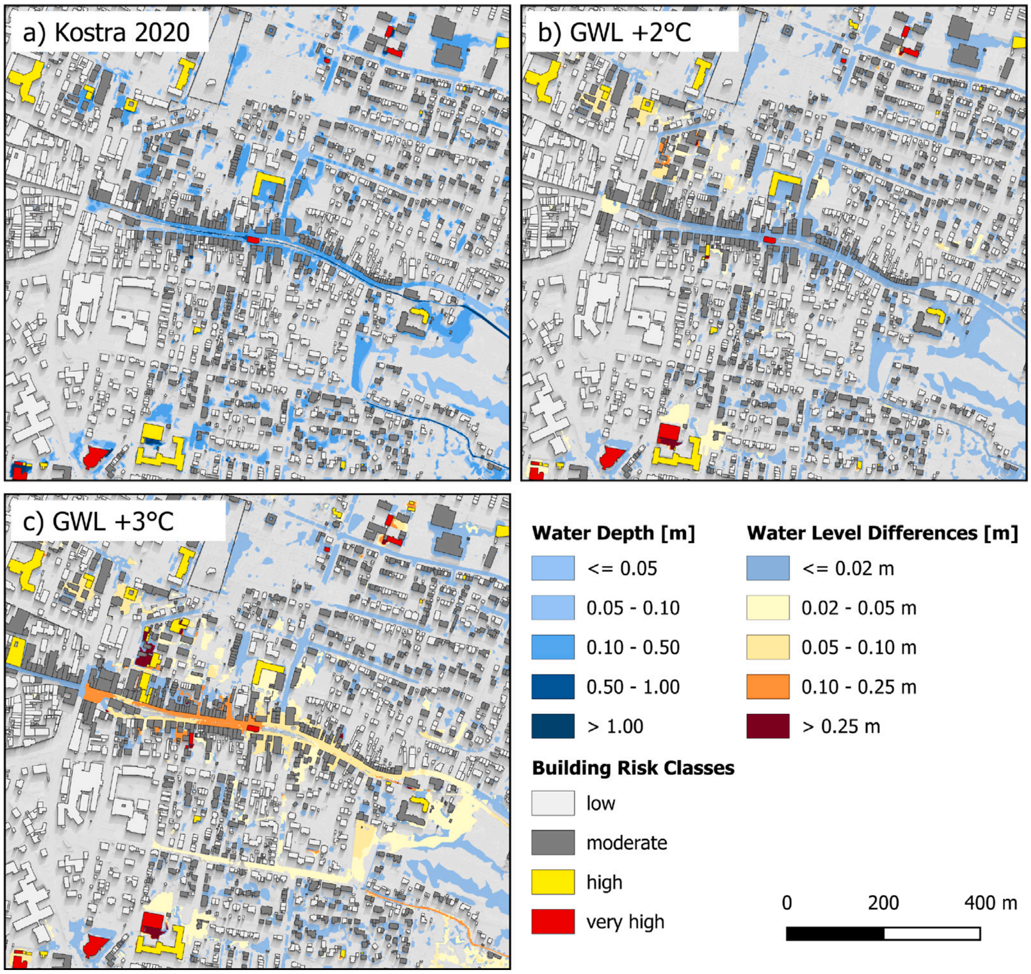

Fig. 7. Inundation areas, illustrated as water depth [m] in Weilheim calculated with the hydrodynamic model, driven by different precipitation scenarios, KOSTRA-DWD (a), GWL +2 °C (b), and GWL +3 °C (c). Figures b and c illustrate the water level differences [m] to the KOSTRA-DWD simulation (a). Furthermore, the individual flood risk of buildings is depicted. The Figure shows only a subset of the model domain.

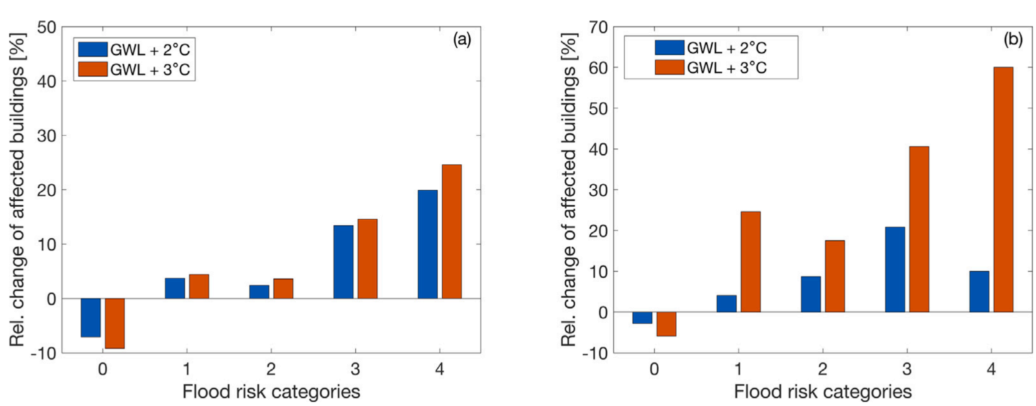

Fig. 8. Relative changes in flood risk under +2 °C and +3 °C GWL scenarios for Garmisch-Partenkirchen (a) and Weilheim (b), both located in the pre-alpine region of Bavaria (southern Germany), compared to the stationary hydraulic assessment based on KOSTRA-DWD. Flood risk categories are explained in Table 1.

We analyzed the impact of the expected climate change by conducting high-resolution and computationally demanding hydrodynamic flood modeling (Figs. 6 and 7) at the commune level in a hot spot region, characterized by enhanced hourly precipitation extremes and climate sensitivity, i.e., prevailing high precipitation extreme values and high differences between the +2 °C and +3 °C GWL scenarios. While higher risks up to 60% for the highest risk classes are found between the historical and the future climate conditions (see Fig. 8), differences up to 50% between the two different GWL scenarios can be observed for Weilheim (highest risk class).

In this study, the uncertainties stem from different sources, such as the climate modeling, the model parameters of the TENAX and the hydrodynamic models, and the different observational datasets applied (see Section 2 for details on each component of the CHMC). While high uncertainties can be expected particularly for short-duration extreme events and long return periods (Hosseinzadehtalaei et al.,

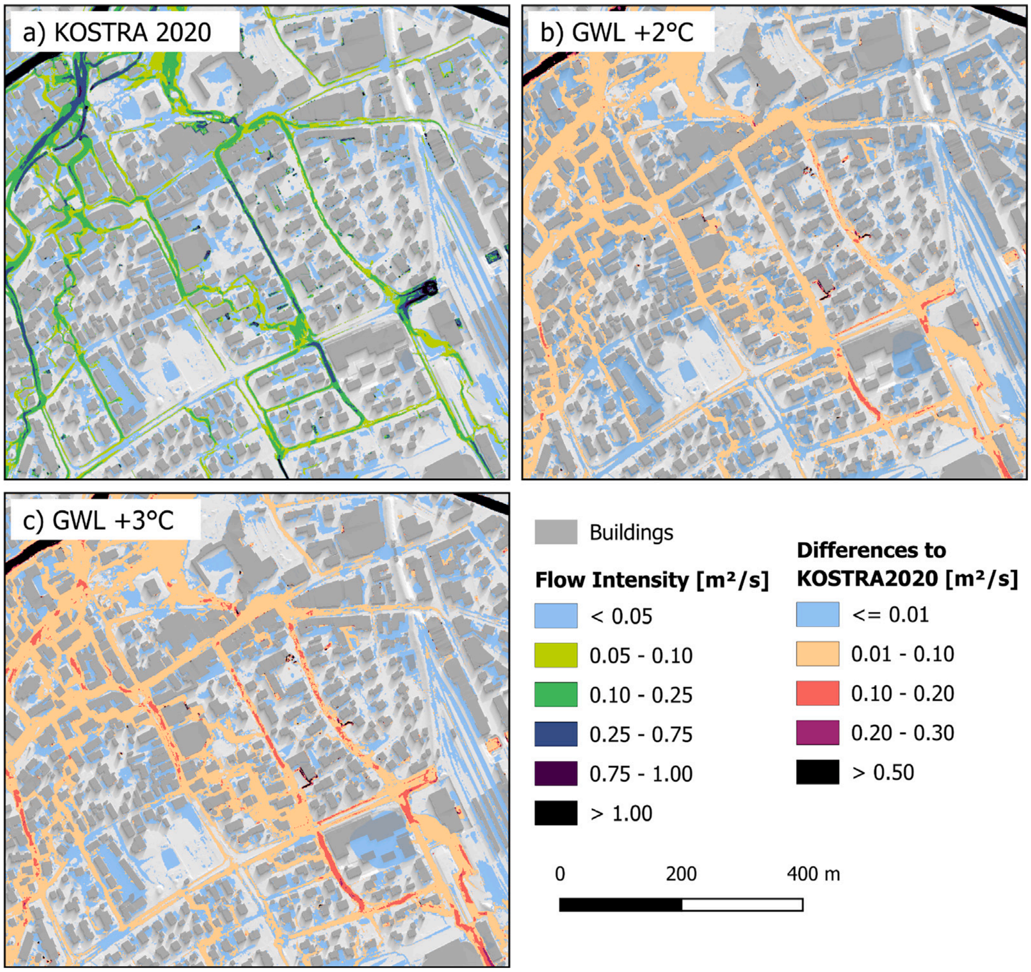

Fig. 9. Flow intensity differences [m^2/s] in Garmisch-Partenkirchen calculated with the hydrodynamic model, driven by different precipitation scenarios, KOSTRA-DWD Version 2020 (a), GWL +2 °C (b) and GWL +3 °C (b). Figures b and c illustrate the flow intensity differences [m] to the KOSTRA-DWD simulation (a). The Figure shows only a subset of the model domain.

2018, 2020), as it is the focus of this study, the quantification of the overall uncertainties, including the uncertainties contributed from each source is virtually impossible due to the complexity of the CHMC and the computational demands of the single components. For example, the computational demands for the German-wide assessment of hourly precipitation extremes restricted the application of the TENAX model to the NUKLEUS CPM ensemble mean statistics of the +2 °C and the +3 °C scenario. This prohibits a dedicated uncertainty quantification of the climate input. However, it is well-recognized that high uncertainty results from the climate boundary conditions (Jeantet et al., 2023). Due to the applied GWL approach of the GCM/RCM ensemble, the uncertainty stemming from different emission trajectories could be partly reduced (Evin et al., 2024). Within the TENAX model, an uncertainty estimation of extreme precipitation values has been conducted for selected grid cells based on bootstrap sampling, however, a German-wide assessment has been omitted due to computational reasons. Demanding hydrodynamic model simulations at the end of the CHMC would prevent us from assessing the propagation of these uncertainties to the hydrodynamic risk assessment.

Despite significant uncertainties in the CHMC, a consistent European study remains highly desirable (Hosseinzadehtalaei et al., 2020). The application of the TENAX model helps mitigate the challenges posed by short time series and offers a robust framework for deriving projections of future IDF values based on temperature shifts (Marra et al., 2024). However, the progress is currently hindered by the limited availability of dense, sub-daily precipitation data, both from observations and CPM simulations (Hundhausen et al., 2024; Dallan et al., 2022; Prein et al., 2017; Sun et al., 2021; Hundhausen et al., 2024; Poschlod, 2021).

Unlike city-scale future design storm values, such as the ones presented by Peleg et al. (2024), this study derives 1-h precipitation design levels for a 100-year return period under two future climate scenarios for the whole of Germany for the first time (available under Laux (2024)), encouraging further process-based hydraulic projections for pluvial flooding in German urban catchments.

Due to the current data limitations for the whole of Europe, the presented CHMC may serve as a blueprint for a county-wide assessment of future design storm values with similar data infrastructures (radar data, observations, and CPM simulations).

5. Conclusion

We hypothesize that future short-duration extreme rainfall events may lead to higher inundation levels compared to the events currently used as a standard in engineering. Assessing future hourly precipitation extremes using the TENAX model and high-resolution observational and CPM data for the whole of Germany (i.e., RADKLIM, HYRAS, and NUKLEUS), we derived future hourly precipitation extremes for +2 °C and +3 °C GWL scenarios. Hydrodynamic simulations for two German municipalities reveal that with climate change, our current approaches significantly underestimate flood risk. Similar impacts are likely in other regions, particularly in southern Germany, where the highest increases in 1-h precipitation extremes are expected. These findings suggest that critical infrastructure designed with the standard approach

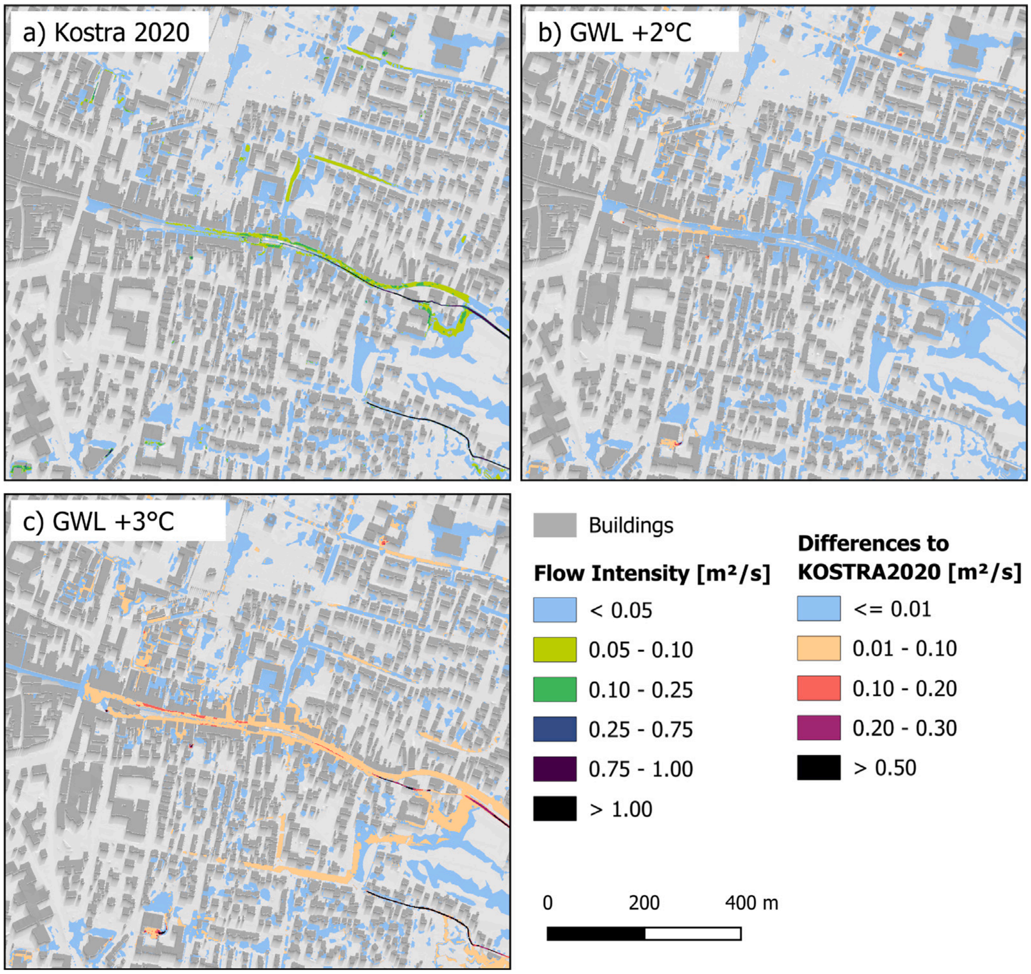

Fig. 10. Flow intensity differences [m^2/s] in Weilheim calculated with the hydrodynamic model, driven by different precipitation scenarios, KOSTRA-DWD Version 2020 (a), GWL +2 °C (b) and GWL +3 °C (b). Figures b and c illustrate the flow intensity differences [m] to the KOSTRA-DWD simulation (a). The Figure shows only a subset of the model domain.

might be ill-prepared for flooding in a +2 °C or +3 °C warmer world. To support climate-resilient adaptation, we provide high-resolution future hourly precipitation extremes with a 100-year return level (Laux, 2024) to scientists, engineers, and water managers. The presented CHMC framework may serve as a blueprint for other countries with similar data infrastructures.

CRediT authorship contribution statement

Patrick Laux: Writing – original draft, Visualization, Validation, Supervision, Software, Resources, Project administration, Methodology, Investigation, Funding acquisition, Formal analysis, Data curation, Conceptualization. **David Feldmann:** Writing – review & editing, Writing – original draft, Visualization, Software, Methodology, Conceptualization. **Francesco Marra:** Writing – review & editing, Writing – original draft, Methodology, Conceptualization. **Hendrik Feldmann:** Writing – review & editing, Writing – original draft, Methodology, Data curation. **Harald Kunstmann:** Writing – review & editing. **Katja Trachte:** Writing – review & editing, Data curation. **Nadav Peleg:** Writing – original draft, Methodology, Conceptualization.

Declaration of competing interest

FM and NP are members of the editorial board of the Journal of Hydrology.

Acknowledgments

The authors thank the DWD for providing various datasets (KOSTRA-DWD, HYRAS, RADKLIM). Data about sewer networks are provided by the local Municipal Building Authorities of Garmisch-Partenkirchen and Weilheim. We also thank the DKRZ for providing storage resources at WDCC, and KIT/IMK-IFU for providing computing facilities. Special thanks to Benjamin Fersch and Frank Neidl for the maintenance of the Linux Cluster as well as to Christoph Braun (KIT) and Christian Beier (BTU) for their help on Figures S1, S2, and S3. We thank the BMBF for funding the KARE (phase 1, grant 01LR2006D) and the NUKLEUS project (phase 1 grant 01LR2002B/E) for conducting CPM simulations. NP was supported by the Swiss National Science Foundation (SNSF), Grant 194649 ("Rainfall and floods in future cities"). FM was funded within the Project "The Geosciences for Sustainable Development" project (Budget Ministero dell'Università e della Ricerca–Dipartimenti di Eccellenza 2023–2027 C93C23002690001).

Appendix A. Supplementary data

Supplementary material related to this article can be found online at https://doi.org/10.1016/j.jhydrol.2025.133607.

Data availability

Data from the NUKLEUS CPM ensemble can be obtained from https://www-regiklim.dkrz.de/?login_required=1&next=/solr/data-browse

r/%3Fproduct%3Dceu-3%26project%3Dnukleus. KOSTRA (Grids of return periods of heavy precipitation (design precipitation) over Germany (KOSTRA-DWD, Version 2020)), HYRAS-DE-TAS (Version v5.0), and RADKLIM (Version 2017.002) data can be obtained from the Climate Data Center (CDC) at https://opendata.dwd.de/climate_environment/CDC/. The newly generated non-stationary precipitation extreme values are provided at the World Data Center for Climate (WDCC) at DKRZ, under https://www.wdc-climate.de/ui/entry?acronym=PrecExtr100yr, doi:10.26050/WDCC/PrecExtr100yr. The TENAX model is available at https://doi.org/10.5281/zenodo.8332232, and the SMEV model is available at https://doi.org/10.5281/zenodo.3971557.

References

Amponsah, W., Ayral, P.A., Boudevillain, B., Bouvier, C., Braud, I., Brunet, P., Delrieu, G., DIdon-Lescot, J.F., Gaume, E., Lebouc, L., Marchi, L., Marra, F., Morin, E., Nord, G., Payrastre, O., Zoccatelli, D., Borga, M., 2018. Integrated high-resolution dataset of high-intensity European and Mediterranean flash floods. Earth Syst. Sci. Data 10, 1783–1794. http://dx.doi.org/10.5194/essd-10-1783-2018.

Ban, N., Schmidli, J., Schär, C., 2015. Heavy precipitation in a changing climate: Does short-term summer precipitation increase faster?. Geophys. Res. Lett. 42, 1165–1172. http://dx.doi.org/10.1002/2014GL062588.

Berthou, S., Kendon, E.J., Chan, S.C., Ban, N., Leutwyler, D., Schär, C., Fosser, G., 2020. Pan-European climate at convection-permitting scale: a model intercomparison study. Clim. Dyn. 55, 35–59. http://dx.doi.org/10.1007/s00382-018-4114-6.

Borga, M., Comiti, F., Ruin, I., Marra, F., 2019. Forensic analysis of flash flood response. Wiley Interdiscip. Rev.: Water 6, 1–9. http://dx.doi.org/10.1002/wat2.1338.

Bronstert, A., Agarwal, A., Boessenkool, B., Crisologo, I., Fischer, M., Heistermann, M., Köhn-Reich, L., López-Tarazón, J.A., Moran, T., Ozturk, U., Reinhardt-Imjela, C., Wendi, D., 2018. Forensic hydro-meteorological analysis of an extreme flash flood: The 2016-05-29 event in Braunsbach, SW Germany. Sci. Total Environ. 630, 977–991. http://dx.doi.org/10.1016/j.scitotenv.2018.02.241.

Bürger, M., Bronstert, A., 2014. Towards subdaily rainfall disaggregation via Clausius – Clapeyron. http://dx.doi.org/10.1175/JHM-D-13-0161.1.

Cannon, A.J., 2025. Twelve months at 1.5°C signals earlier than expected breach of Paris Agreement threshold. Nat. Clim. Chang. 15, 266–269. http://dx.doi.org/10.1038/s41558-025-02247-8.

Clark, P., Roberts, N., Lean, H., Ballard, S.P., Charlton-Perez, C., 2016. Convection-permitting models: A step-change in rainfall forecasting. Meteorol. Appl. 23, 165–181. http://dx.doi.org/10.1002/met.1538.

Da Silva, N.A., Haerter, J.O., 2023. The Precipitation Characteristics of Mesoscale Convective Systems Over Europe. J. Geophys. Res.: Atmos. 128, http://dx.doi.org/10.1029/2023JD039045.

Dallan, E., Borga, M., Fosser, G., Canale, A., Roghani, B., Marani, M., Marra, F., 2024a. A Method to Assess and Explain Changes in Sub-Daily Precipitation Return Levels From Convection-Permitting Simulations. Water Resour. Res. 60, http://dx.doi.org/10.1029/2023WR035969.

Dallan, E., Borga, M., Zaramella, M., Marra, F., 2022. Enhanced Summer Convection Explains Observed Trends in Extreme Subdaily Precipitation in the Eastern Italian Alps. Geophys. Res. Lett. 49, http://dx.doi.org/10.1029/2021GL096727.

Dallan, E., Marra, F., Fosser, G., Marani, M., Borga, M., 2024b. Dynamical factors heavily modulate the future increase of Sub-Daily extreme precipitation in the Alpine - Mediterranean Region Earth's Future. pp. 1–16. http://dx.doi.org/10.1029/2024EF005185.

Dang, Q., Laux, P., Kunstmann, H., 2017. Future high- and low-flow estimations for Central Vietnam: a hydro-meteorological modelling chain approach. Hydrol. Sci. J. 62, 1867–1889. http://dx.doi.org/10.1080/02626667.2017.1353696.

DVWK, 1999. HochwasserabflÜsse / [Hrsg.: Deutscher Verband FÜr Wasserwirtschaft Und Kulturbau E.V. (DVWK)]. In: Schriftenreihe des Deutschen Verbandes für Wasserwirtschaft und Kulturbau e.V, Vol. 124, Wirtschafts- und Verl.-Ges. Gas und Wasser, Bonn.

EC-Earth-Consortium, 2019a. EC-Earth3-veg model output prepared for CMIP6 CMIP historical. http://dx.doi.org/10.22033/ESGF/CMIP6.4706.

EC-Earth-Consortium, 2019b. EC-Earth3-veg model output prepared for CMIP6 scenarioMIP ssp370. http://dx.doi.org/10.22033/ESGF/CMIP6.4886.

Evin, G., Ribes, A., Corre, L., 2024. Assessing CMIP6 uncertainties at global warming levels. Clim. Dyn. http://dx.doi.org/10.1007/s00382-024-07323-x.

Feldmann, D., Laux, P., Heckl, A., Schindler, M., Kunstmann, H., 2023. Near surface roughness estimation : A parameterization derived from artificial rainfall experiments and two-dimensional hydrodynamic modelling for multiple vegetation coverages. J. Hydrol. 617, 128786. http://dx.doi.org/10.1016/j.jhydrol.2022.128786.

Fosser, G., Adinolfi, M., Ban, N., Belušić, C., Cardoso, R., Coppola, E., Demory, M.E., Vries, H.De., Dobler, A., Feldmann, H., Gaetani, M., Görgen, E., Lenderink, G., Pichelli, E., Schär, P.M., Somot, S., Tölle, M.H., 2024. Convection-permitting climate models offer more certain extreme rainfall projections. npj Clim Atmos Sci 7, 51. http://dx.doi.org/10.1038/s41612-024-00600-w.

Fowler, H.J., Wasko, C., Prein, A.F., 2021a. Intensification of short-duration rainfall extremes and implications for flood risk: Current state of the art and future directions. Philos. Trans. R. Soc. A: Math. Phys. Eng. Sci. 379, http://dx.doi.org/10.1098/rsta.2019.0541.

Fowler, H.J., Wasko, C., Prein, A.F., 2021b. Intensification of short-duration rainfall extremes and implications for flood risk: Current state of the art and future directions. Philos. Trans. R. Soc. A: Math. Phys. Eng. Sci. 379, http://dx.doi.org/10.1098/rsta.2019.0541.

Guerreiro, S.B., Fowler, H.J., Barbero, R., Westra, S., Lenderink, G., Blenkinsop, S., Lewis, E., Li, X.F., 2018. Detection of continental-scale intensification of hourly rainfall extremes. Nat. Clim. Chang. 8, 803–807. http://dx.doi.org/10.1038/s41558-018-0245-3.

Hosseinzadehtalaei, P., Tabari, H., Willems, P., 2018. Precipitation intensity–duration–frequency curves for central Belgium with an ensemble of EURO-CORDEX simulations, and associated uncertainties. Atmos. Res. 200, 1–12. http://dx.doi.org/10.1016/j.atmosres.2017.09.015.

Hosseinzadehtalaei, P., Tabari, H., Willems, P., 2020. Climate change impact on short-duration extreme precipitation and intensity–duration–frequency curves over Europe. J. Hydrol. 590, 125249. http://dx.doi.org/10.1016/j.jhydrol.2020.125249.

Hundhausen, M., Feldmann, H., Kohlhepp, R., Pinto, J.G., 2024. Climate change signals of extreme precipitation return levels for Germany in a transient convection-permitting simulation ensemble. Int. J. Climatol. 1–18. http://dx.doi.org/10.1002/joc.8393.

Hundhausen, M., Feldmann, H., Laube, N., Pinto, J.G., 2023. Future heat extremes and impacts in a convection-permitting climate ensemble over Germany. Nat. Hazards Earth Syst. Sci. 23, 2873–2893. http://dx.doi.org/10.5194/nhess-23-2873-2023.

Hydrotec, 2023. Hydroas - 2D-flow model for water management applications - reference manual.

Jeantet, A., Thirel, G., Lemaitre-Basset, T., Tournebize, J., 2023. Uncertainty propagation in a modelling chain of climate change impact for a representative French drainage site. Hydrol. Sci. J. 68, 1426–1442. http://dx.doi.org/10.1080/02626667.2023.2203322.

Jungclaus, J., Bittner, M., Wieners, K.H., Wachsmann, F., Schupfner, M., Legutke, S., Giorgetta, M., Reick, C., Gayler, V., Haak, H., de Vrese, P., Raddatz, T., Esch, M., Mauritsen, T., von Storch, J.S., Behrens, J., Brovkin, V., Claussen, M., Crueger, T., Fast, I., Fiedler, S., Hagemann, S., Hohenegger, C., Jahns, T., Kloster, S., Kinne, S., Lasslop, G., Kornblueh, L., Marotzke, J., Matei, D., Meraner, K., Mikolajewicz, U., Modali, K., Müller, J., Notz, D., Peters-von Gehlen, K., Pincus, R., Pohlmann, H., Pongratz, J., Rast, S., Schmidt, H., Schnur, R., Schulzweida, U., Six, K., Stevens, B., Voigt, A., Roeckner, E., 2019. MPI-M MPI-ESM1.2-HR model output prepared for CMIP6 CMIP historical. http://dx.doi.org/10.22033/ESGF/CMIP6.6594.

Junghänel, T., Ertel, H., Deutschländer, T., Wetterdienst, D., Hydrometeorologie, A., 2017. Bericht zur Revision der koordinierten Starkregenregionalisierung und-auswertung des Deutschen Wetterdienstes in der Version 2010. Technical Report, URL: https://www.dwd.de/DE/leistungen/kostra_dwd_rasterwerte/download/bericht_revision_kostra_dwd_2010.pdf?_blob=publicationFile&v=6.

Kron, W., Löw, P., Kundzewicz, Z.W., 2019. Changes in risk of extreme weather events in Europe. Environ. Sci. Policy 100, 74–83. http://dx.doi.org/10.1016/j.envsci.2019.06.007.

Laux, P., 2024. Modelled non-stationary kilometer-scale hourly precipitation extremes of a 100-year event under 2 GWL scenarios for Germany. http://dx.doi.org/10.26050/WDCC/PrecExtr100yr.

Laux, P., Rötter, H., Dieng, D., Rahimi, J., Wei, J., Faye, B., Srivastana, A., Bliefernicht, J., Adeyeri, O., Arnault, J., Kunstmann, H., 2021. To bias correct or not to bias correct? An agricultural impact modelers' perspective on regional climate model data. Agricult. Forest. Meterol. 304–305, 108406. http://dx.doi.org/10.1016/j.agrformet.2021.108406.

Laux, P., Weber, E., Feldmann, D., Kunstmann, H., 2023. The robustness of the derived design life levels of heavy precipitation events in the Pre-Alpine Oberland Region of southern Germany. Atmosphere http://dx.doi.org/10.3390/atmos14091384.

Lengfeld, K., Kirstetter, P.E., Fowler, H.J., Yu, J., Becker, A., Flamig, Z., Gourley, J., 2020. Use of radar data for characterizing extreme precipitation at fine scales and short durations. Environ. Res. Lett. 15, http://dx.doi.org/10.1088/1748-9326/ab98b4.

Lengfeld, K., Marra, F., 2024. Estimation of design precipitation using weather radar in Germany: A comparison of statistical methods. J. Hydrol.: Reg. Stud. 55, http://dx.doi.org/10.1016/j.ejrh.2024.101952.

Lengfeld, K., Winterrath, T., Jungh, T., Hafer, M., Becker, A., 2019. Characteristic spatial extent of hourly and daily precipitation events in Germany derived from 16 years of radar data. Meteorol. Z. 28 (5), 363–378.

LfU, 2017. Sturzfluten- Und Hochwasserereignisse Mai/Juni 2016. Wasserwirtschaftlicher Bericht.

LfU-Bayern, 2022. Leitfaden Zur Aufstellung Von Konzepten Zum Kommunalen Sturzflut-Risikomanagement. Technical Report.

Ludwig, P., Ehmele, F., Franca, M.J., Mohr, S., Caldas-Alvarez, A., Daniell, J.E., Ehret, U., Feldmann, H., Hundhausen, M., Knippertz, P., Küpfer, M., Mühr, J.G., Quinting, J., Schäfer, A.M., Seidel, F., Wisotzky, C., 2023. A multi-disciplinary analysis of the exceptional flood event of 2021 in central Europe - Part 2: Historical context and relation to climate change. Nat. Hazards Earth Syst. Sci. 23, 1287–1311. http://dx.doi.org/10.5194/nhess-23-1287-2023.

Marra, F., Borga, M., Morin, E., 2020. A Unified Framework for Extreme Subdaily Precipitation Frequency Analyses Based on Ordinary Events. Geophys. Res. Lett. 47, 1–8. http://dx.doi.org/10.1029/2020GL090209.

Marra, F., Koukoula, M., Canale, A., Peleg, N., 2024. Predicting extreme sub-hourly precipitation intensification based on temperature shifts. Hydrol. Earth Syst. Sci. 28, 375–389. http://dx.doi.org/10.5194/hess-28-375-2024.

Marra, F., Zoccatelli, D., Armon, M., Morin, E., 2019. A simplified MEV formulation to model extremes emerging from multiple nonstationary underlying processes. Adv. Water Resour. 127, 280–290. http://dx.doi.org/10.1016/j.advwatres.2019.04.002.

Masson-Delmotte, V., Zhai, P., Pirani, A., Connors Sarah, L., Clotilde, Péan, Yang, Chen, Leah, Goldfarb, Gomis Melissa, I., Robin, Matthews J.B., Sophie, Berger, Mengtian, Huang, Ozge, Yelekçi, Rong, Yu, Baiquan, Zhou, Elisabeth, Lonnoy, Maycock Thomas, K., Tim, Waterfield, Katherine, Leitzell, Nada, Caud, 2021. Summary for policymakers. In: Climate Change 2021: The Physical Science Basis. Contribution of Working Group I to the Sixth Assessment Report of the Intergovernmental Panel on Climate Change. Cambridge University Press, Cambridge, United Kingdom and New York, NY, USA, http://dx.doi.org/10.1017/9781009157896.001.

Milly, P.C., Betancourt, J., Falkenmark, M., Hirsch, R.M., Kundzewicz, Z.W., Lettenmaier, D.P., Stouffer, R.J., 2008. Climate change: Stationarity is dead: Whither water management? Science 319, 573–574. http://dx.doi.org/10.1126/science.1151915.

Nimac, I., Cindrić Kalin, K., Renko, T., Vujnović, T., Horvath, K., 2022. The analysis of summer 2020 urban flood in Zagreb (Croatia) from hydro-meteorological point of view. Nat. Hazards 112, 873–897. http://dx.doi.org/10.1007/s11069-022-05210-4.

Ochoa-Rodriguez, S., Wang, L.P., Gires, A., Pina, R.D., Reinoso-Rondinel, R., Bruni, G., Ichiba, A., Gaitan, S., Cristiano, E., Assel, J.Van., Kroll, S., Murlà-Tuyls, .B., Schertzer, D., Tchiguirinskaia, I., Onof, C., Willems, P., Ten Veldhuis, M.C., 2015. Impact of spatial and temporal resolution of rainfall inputs on urban hydrodynamic modelling outputs: A multi-catchment investigation. J. Hydrol. 531, 389–407. http://dx.doi.org/10.1016/j.jhydrol.2015.05.035.

Peleg, N., Ban, N., Gibson, M.J., Chen, A.S., Paschalis, A., Burlando, P., Leitão, J.P., 2022. Mapping storm spatial profiles for flood impact assessments. Adv. Water Resour. 166, 104258. http://dx.doi.org/10.1016/j.advwatres.2022.104258.

Peleg, N., Wright, D.B., Fowler, H.J., Leitão, A., Marra, F., 2024. A simple and robust approach for adapting design storms to assess climate-induced changes in flash flood hazard. Adv. Water Resour. 193, 104823. http://dx.doi.org/10.1016/j.advwatres.2024.104823, URL: https://linkinghub.elsevier.com/retrieve/pii/S0309170824002100.

Persiano, S., Ferri, E., Antolini, G., Domeneghetti, A., Pavan, V., Castellarin, A., 2020. Changes in seasonality and magnitude of sub-daily rainfall extremes in Emilia-Romagna (Italy) and potential influence on regional rainfall frequency estimation. J. Hydrol.: Reg. Stud. 32, http://dx.doi.org/10.1016/j.ejrh.2020.100751.

Piper, D., Kunz, M., Ehmele, F., Mohr, S., Mühr, A., Daniell, J., 2016. Exceptional sequence of severe thunderstorms and related flash floods in May and 2016 in Germany - Part 1: Meteorological background. Nat. Hazards Earth Syst. Sci. 16, 2835–2850. http://dx.doi.org/10.5194/nhess-16-2835-2016.

Pironneau, O., 1988. Finite Element Methods for Fluids. Wiley, Paris.

Poschlod, B., 2021. Using high-resolution regional climate models to estimate return levels of daily extreme precipitation over Bavaria. Nat. Hazards Earth Syst. Sci. 21, 3573–3598. http://dx.doi.org/10.5194/nhess-21-3573-2021.

Pöschmann, J.M., Kim, D., Kronenberg, R., Bernhofer, C., 2021. An analysis of temporal scaling behaviour of extreme rainfall in Germany based on radar precipitation QPE data. Nat. Hazards Earth Syst. Sci. 21, 1195–1207. http://dx.doi.org/10.5194/nhess-21-1195-2021.

Prein, A.F., Rasmussen, R.M., Ikeda, K., Liu, C., Clark, M.P., Holland, .G.J., 2017. The future intensification of hourly precipitation extremes. Nat. Clim. Chang. 7, 48–52. http://dx.doi.org/10.1038/nclimate3168.

Razafimaharo, C., Krähenmann, S., Höpp, S., Rauthe, M., Deutschländer, T., 2020. New high-resolution gridded dataset of daily mean, minimum, and maximum temperature and relative humidity for Central Europe (HYRAS). Theor. Appl. Climatol. 142, 1531–1553. http://dx.doi.org/10.1007/s00704-020-03388-w.

Samela, C., Persiano, S., Bagli, S., Luzzi, V., Mazzoli, P., Humer, G., Reithofer, A., Essenfelder, A., Amadio, M., Mysiak, J., Castellarin, A., 2020. Safer _ RAIN : A DEM-Based Hierarchical Urban Areas. Water 12, 1514.

Schupfner, M., Wieners, K.H., Wachsmann, F., Steger, C., Bittner, M., Jungclaus, J., Früh, K., Giorgetta, M., Reick, C., Legutke, S., Esch, M., Gayler, V., Haak, H., Vrese, P.de., Raddatz, T., Mauritsen, T., von Storch, J.S., Behrens, J., Brovkin, V., Claussen, M., Crueger, T., Fast, I., Fiedler, S., Hagemann, S., Hohenegger, C., Jahns, T., Kloster, S., Kinne, S., Lasslop, G., Kornblueh, L., Marotzke, J., Matei, D., Meraner, K., Mikolajewicz, U., Modali, K., Müller, J., Notz, D., Gehlen, K. Peters-von., Pincus, R., Pohlmann, H., Pongratz, J., Rast, S., Schmidt, H., Schnur, R., Schulzweida, U., Six, K., Stevens, B., Voigt, A., Roeckner, E., 2019. DKRZ MPI-ESM1.2-HR model output prepared for CMIP6 ScenarioMIP ssp370. http://dx.doi.org/10.22033/ESGF/CMIP6.4399.

Sharma, A., Wasko, C., Lettenmaier, D.P., 2018. If Precipitation Extremes Are Increasing, Why Aren't Floods? Water Resour. Res. 54, 8545–8551. http://dx.doi.org/10.1029/2018WR023749.

Shiogama, H., Abe, M., Tatebe, H., 2019. MIROC MIROC6 model output prepared for CMIP6 ScenarioMIP ssp370. http://dx.doi.org/10.22033/ESGF/CMIP6.5752.

Shrestha, M., Acharya, S.C., Shrestha, P.K., 2017. Bias correction of climate models for hydrological modelling – are simple methods still useful? Meteorol. Appl. 24, 531–539. http://dx.doi.org/10.1002/met.1655.

Sobolowski, S., Somot, S., Fernandez, J., Evin, G., Maraun, D., Kotlarski, S., Jury, M., Benestad, R.E., Teichmann, C., Christensen, O.B., Katharina, B., Buonomo, E., Katragkou, E., Steger, C., Sørland, S.L., Nikulin, G., McSweeney, C.F., Dobler, A., Palmer, T.N., Brands, S., 2023. EURO-CORDEX GCM Selection & Ensemble Design: Implementation Framework. Zenodo, http://dx.doi.org/10.5281/zenodo.7673400.

Sørland, S.L., Brogli, R., Pothapakula, P.K., Russo, E., Walle, J.Van.De., Ahrens, B., Anders, I., Bucchignani, E., Davin, E.L., Demory, M.E., Dosio, A., Feldmann, H., Früh, B., Keuler, K., Lee, D., Li, D., Van Lipzig, N.P., Min, S.K., Panitz, H.J., Rockel, B., Schär, C., Steger, C., Thiery, W., 2021. COSMO-CLM regional climate simulations in the Coordinated Regional Climate Downscaling Experiment (CORDEX) framework: A review. Geosci. Model. Dev. 14, 5125–5154. http://dx.doi.org/10.5194/gmd-14-5125-2021.

Sun, Q., Zhang, X., Zwiers, F., Westra, S., Alexander, L.V., 2021. A global, continental, and regional analysis of changes in extreme precipitation. J. Clim. 34, 243–258. http://dx.doi.org/10.1175/JCLI-D-19-0892.1.

Tan, W.Y., 1992. Shallow Water Hydrodynamics - Mathematical Theory and Numerical Solution for a Two-Dimensional System of Shallow Water Equations, first ed..

Tatebe, H., Watanabe, M., 2018. MIROC MIROC6 model output prepared for CMIP6 CMIP historical. http://dx.doi.org/10.22033/ESGF/CMIP6.5603.

Teichmann, C., Bülow, K., Otto, J., Pfeifer, S., Rechid, D., Sieck, K., Jacob, D., 2018. Avoiding extremes: Benefits of staying below +1.5 °C compared to +2.0 °C and +3.0 °C global warming. Atmosphere 9, 1–19. http://dx.doi.org/10.3390/atmos9040115.

Trenberth, K.E., Dai, A., Rasmussen, R.M., Parsons, D.B., 2003. The changing character of precipitation. Bull. Am. Meteorol. Soc. 84, 1205–1217. http://dx.doi.org/10.1175/BAMS-84-9-1205.

United Nations Environment Programme, 2024. Emissions Gap Report 2024: No more Hot Air ...Please!. United Nations Environment Programme, URL: https://www.unep.org/resources/emissions-gap-report-2024.

USDA National Resources Conservation Service, 2004. National Engineering HAndbook: Part 630—Hydrology. U.S. Dep. of Agric. Nat. Resour.Conserv. Serv.

Van Pham, T., Steger, C., Rockel, B., Keuler, K., Kirchner, I., Mertens, M., Rieger, D., Zäng, G., Früh, B., 2021. Icon in climate limited-Area mode (icon release version 2.6.1): A new regional climate model. Geosci. Model. Dev. 14, 985–1005. http://dx.doi.org/10.5194/gmd-14-985-2021.

Warner, T.T., 2011. Numerical Weather and Climate Prediction. Cambridge University Press, Cambridge, United Kingdom, http://dx.doi.org/10.1017/CBO9780511763243.

Westra, S., Fowler, H.J., Evans, J.P., Alexander, L.V., Berg, P., Johnson, F., Kendon, E.J., Lenderink, G., Roberts, N.M., 2014. Future changes to the intensity and frequency of short-duration extreme rainfall. http://dx.doi.org/10.1002/2014RG000464.

Winterrath, T., Brendel, T., Junghänel, T., Klameth, A., Lengfeld, K., Walawender, E., Weigl, E., Hafer, M., Becker, A., 2019. An overview of the new radar-based precipitation climatology of the Deutscher Wetterdienst-data, methods, products conference Paper. UrbanRain 18, http://dx.doi.org/10.3929/ethz-b-000347607.

Winterrath, T., Brendel, C.H.M., Junghänel, A., Lengfeld, K., Walawender, E., Weigl, E., Becker, A., 2018. RADKLIM version 2017.002: Reprocessed gauge-adjusted radar data, one-hour precipitation sums (RW).

Zängl, D., Rípodas, P., Baldauf, M., 2015. The ICON (ICOsahedral Non-hydrostatic) modelling framework of DWD and MPI-M: Description of the non-hydrostatic dynamical core. Q. J. R. Meteorol. Soc. 141, 563–579. http://dx.doi.org/10.1002/qj.2378.

Zorzetto, E., Marani, M., Botter, G., 2016. On the emergence of rainfall extremes from ordinary events. Geophys. Res. Lett. 43, 8076–8082. http://dx.doi.org/10.1002/2016GL069445.